Published in final edited form as:

Stem Cells. 2015 February ; 33(2): 468–478. doi:10.1002/stem.1851.

Human Adipose-derived Stem Cells Ameliorate Cigarette Smoke-induced Murine Myelosuppression via TSG-6

Jie Xie[a,b,f], **Hal E. Broxmeyer**[c], **Dongni Feng**[b,f], **Kelly S. Schweitzer**[d], **Ru Yi**[a,b,f], **Todd G. Cook**[b,f], **Brahmananda R. Chitteti**[d], **Daria Barwinska**[a,b,f], **Dmitry O. Traktuev**[b,d,f], **Mary J. Van Demark**[d], **Matthew J. Justice**[d], **Xuan Ou**[c], **Edward F. Srour**[c,d,e], **Darwin J. Prockop**[g], **Irina Petrache**[b,d,f], and **Keith L. March**[a,b,d,f]

[a]Department of Cellular & Integrative Physiology, Indiana University

[b]Indiana Center for Vascular Biology and Medicine, VC-CAST Signature Center, Indiana University

[c]Department of Microbiology and Immunology, Indiana University

[d]Department of Medicine, Indiana University

[e]Department of Pediatrics, and Herman B Wells Center for Pediatric Research, Indiana University

[f]VA Center for Regenerative Medicine Indianapolis, “Richard L. Roudebush” VA Medical Center, Indianapolis, Indiana, USA

[g]Institute for Regenerative Medicine, Texas A&M Health Science Center, Temple, Texas, USA

Abstract

Objective—Bone marrow-derived hematopoietic stem and progenitor cells (HSC/HPC) are critical to homeostasis and tissue repair. The aims of this study were to delineate the myelotoxicity of cigarette smoking (CS) in a murine model, to explore human adipose-derived stem cells (hASC) as a novel approach to mitigate this toxicity, and to identify key mediating factors for ASC activities.

Methods—C57BL/6 mice were exposed to CS with or without i.v. injection of regular or siRNA-transfected hASC. For in vitro experiments, cigarette smoke extract (CSE) was used to mimic the toxicity of CS exposure. Analysis of bone marrow hematopoietic progenitor cells (HPC) were performed both by flow cytometry and colony forming unit assays.

Results—In this study, we demonstrate that as few as three days of CS exposure result in marked cycling arrest and diminished clonogenic capacity of HPC, followed by depletion of phenotypically-defined HSC/HPC. Intravenous injection of hASC substantially ameliorated both

Correspondence: Keith L. March, M.D., Ph.D., VA Center for Regenerative Medicine, 1481 W 10th St. C3105, Indianapolis, IN 46202, USA. Phone: 317-919-2496; Fax: 317-988-9325; kmarch@iupui.edu.

Author contribution summary: J.X. and H.E.B. designed and performed research, analyzed and interpreted data, and wrote the manuscript; D.F., R.Y., T.G.C., B.R.C., D.B., X.O., M.J.V., and M.J.J. performed research; K.S.S., and D.O.T. assisted in project management and editing the manuscript; E.F.S., D.J.P., I.P., and K.L.M. contributed to the experimental design, data interpretation, and editing the manuscript.

Disclosure of Potential Conflicts of Interest: The other authors declare no competing financial interests.

acute and chronic CS-induced myelosuppression. This effect was specifically dependent on the anti-inflammatory factor TSG-6, which is induced from xenografted hASC, primarily located in the lung and capable of responding to host inflammatory signals. Gene expression analysis within bone marrow HSC/HPC revealed several specific signaling molecules altered by CS and normalized by hASC.

Conclusion—Our results suggest that systemic administration of hASC or TSG-6 may be novel approaches to reverse cigarette smoking-induced myelosuppression.

Keywords

Adipose Stem Cells; Hematopoietic progenitors; Toxicity; Xenogeneic stem cell transplantation

Introduction

Mesenchymal stem cells (MSC), especially those residing in the bone marrow, have been established as critical regulators of hematopoiesis[1]. In recent years, adipose-derived mesenchymal stem cells (ASC) have emerged as a particularly feasible form of cell therapy for tissue repair, due to the ready availability of ASC via liposuction. Several reports have described their capability to facilitate normal hematopoiesis, much resembling that of MSC located in BM [2, 3]. However, the efficacy of ASC as a therapy to correct bone marrow dysfunction and key mediators of these effects remain largely unknown. We have found in several studies that the release of paracrine factors by ASC is critical to their activity to ameliorate injury [4, 5].

Cigarette smoking (CS) is a major risk factor for atherosclerotic vascular disease, COPD, and cancer [6-8], and it affects the function of numerous other organs and systems [9-13]. The effect of CS on hematopoietic stem/progenitor cells has been little explored. Clinically, it has been noted that exposure to CS correlates with worse outcomes of patients receiving hematopoietic stem cell (HSC) transplantation, while nicotine leads to inferior developmental colonization of BM by HSC [14, 15]. A direct effect of CS on BM is supported by experimental studies that revealed a reduction of hematopoietic progenitor cells (HPC) after mice were exposed to CS for 3 weeks [16, 17]. However, the chronology of and potential remedies for this CS-induced BM dysfunction remain unknown.

In a model of murine emphysema induced by chronic CS exposure, we serendipitously observed a marked reduction of HPC in addition to typical emphysematous abnormalities in the lung, both of which could be corrected by periodic intravenous (i.v.) injection of murine ASC, which localized predominantly in the lung [18]. This prompted the hypothesis that secretion of one or more factors by ASC mediated an endocrine-like distant effect on hematopoiesis.

The anti-inflammatory factor TSG-6 has been identified as a key secreted mediator of therapeutic effects of BM-derived MSC in the context of myocardial infarction, peritonitis, acute lung injury, and diabetes [19-22]. The effect of TSG-6 on hematopoiesis has not been explored. In this study, we evaluated the chronology of CS-induced myelosuppression, and the activity of xenotransplanted human ASC (hASC), which can translate easily into future

clinical therapy, to counteract the effect of CS on BM. We identified that systemic secretion of TSG-6 by hASC is both necessary and sufficient in this model to account for the reversal of CS-induced myelosuppression by hASC.

Materials and Methods

Cell culture

Human ASC were isolated by liposuction of human subcutaneous adipose tissue of three female donors, as previously described [23]. Briefly, samples were digested in collagenase Type I solution (Worthington Biochemical, Lakewood, NJ, http://www.worthington-biochem.com/) under agitation for 1 hr at 37°C, and centrifuged at 300 g for 8 min to separate the stromal cell fraction (pellet) from adipocytes. The pellets were filtered through 250 μm Nitex filters (Sefar America, Buffalo, NY, http://www.sefar.us/) and treated with red cell lysis buffer (154 mM NH_4Cl, 10 mM $KHCO_3$, and 0.1 mM ethylenediamine-tetraacetic acid). The final pellet was resuspended and cultured in EGM-2MV media (Lonza, Allendale, NJ, http://www.lonza.com/). ASC were passaged when 60-80% confluent and used at passages three to five. To stimulate hASC with proinflammatory cytokines, cells were treated with 20ng/ml TNFα, 20ng/ml IL1β, or 200ng/ml IFNɣ (human or mouse, R&D systems, Minneapolis, MN, http://www.rndsystems.com/) in EBM2 medium for 24 hrs. To generate TNFα-activated hASC conditioned media (ASC-CM), cells were treated with 20 ng/ml recombinant human TNFα (R&D systems, Minneapolis, MN, http://www.rndsystems.com/) for 24 hrs, washed twice with phosphate buffered saline (PBS), and incubated with fresh EBM2 media (Lonza) for another 24 hrs before collection of ASC-CM. For in vivo administration, concentrated ASC-CM from 3×10^5 hASC was diluted 1:10 in PBS to the injection volume (150ul/mouse, i.v.).

To identify potential engrafted hASC in recipient mouse BM, total BM cells were harvested from both femurs and plated for 7 days in DMEM/10%FBS. Adherent cells were stained with anti-human nuclei antibody (Millipore, Billerica, MA, http://www.millipore.com/).

Animals

Animal studies were approved by the Animal Care and Use Committee of Indiana University. As previously described [18], mice were exposed to 11% mainstream and 89% side-stream smoke from reference cigarettes (3R4F; Tobacco Research Institute, http://www2.ca.uky.edu/) using a Teague 10E whole body exposure apparatus (Teague Enterprises, Woodland, CA, http://www.teague-ent.com/). The exposure chamber atmosphere was monitored for total suspended particulates (average, 90 mg/m^3) and carbon monoxide (average, 350 ppm). For short-term exposure, C57BL/6 (female, age 6-8 wks, Jackson Laboratories, Bar Harbor, Maine, http://www.jax.org/) mice were exposed to CS for 3 days (5 hrs/day). A single i.v. dose of 3×10^5 hASC, ASC-CM, or 2 μg recombinant human TSG-6 (rhTSG-6, R&D systems) was injected (tail vein) on Day 2 of 3-day CS. PBS was used as a control vehicle. For intermediate-term exposure, C57BL/6 mice were exposed to CS for 7 weeks (5 hrs/day, 5 days/week) and received weekly i.v. injections of 3×10^5 hASC. In long-term exposure studies, NOD.Cg-Prkdcscid Il2rgtm1Wjl/SzJ (NSG, Indiana

University) mice were exposed to CS for 6 months (5 hrs/day, 5 days/week) and received weekly i.v. injection of 3×10^5 hASC starting from third month of CS (Figure S3).

CS Extract Preparation

An aqueous CS extract was prepared from filtered research-grade cigarettes (3R4F; Tobacco Research Institute). A stock (100%) CS extract was prepared by bubbling smoke from two cigarettes into 20 ml of PBS at a rate of one cigarette per minute to 0.5 cm above the filter, as previously described [18]. The extract pH was adjusted to 7.4, followed by filtration (0.2 mm, 25 mm, Acrodisc) and used within 20 min. A similar procedure was used to prepare the control extract, replacing the CS with ambient air.

Clonogenic Progenitor Cell Assay

BM samples from C57BL/6 mice were assessed for HPC including granulocyte-macrophage colony-forming unit (CFU-GM), erythroid burst-forming unit (BFU-E), and multipotential granulocyte, erythroid, monocyte, megakaryocyte colony-forming units (CFU-GEMM), as previously described [24, 25]. BM cells were flushed from both femurs. Mononuclear cells were counted using a Hemavet 950FS (Drew Scientific, Dallas, TX, http://www.drew-scientific.com/) and plated at 5×10^4 cells/ml in 0.9% methylcellulose culture medium with 30% FBS (Thermo Fisher Scientific, Waltham, MA, https://www.thermofisher.com/), and 1 U/ml recombinant human erythropoietin (Epo, Amgen Corp, Thousand Oaks, CA, http://www.amgen.com/), 50 ng/ml recombinant murine stem cell factor (rmuSCF, R&D systems), 2 mM glutamine (Cambrex Bio Science, East Rutherford, NJ, http://www.cambrex.com/), 10^{-4} M 2-mercaptoethanol (Thermo Fisher Scientific), 0.1 mM hemin (Sigma-Aldrich, St. Louis, MO, http://www.sigmaaldrich.com/) and 5% vol./vol. pokeweed mitogen mouse spleen cell conditioned medium.[32] For *in vitro* CSE toxicity assays evaluating CFU-GM only, 5×10^4 murine BM mononuclear cells were plated and cultured in 0.3% methylcellulose culture medium in the presence of 50 ng/mL rmuSCF and 10 ng/mL recombinant murine GM-CSF (rmuGM-CSF, R&D systems). Absolute HPC numbers were calculated from the nucleated cell counts per femur and the number of colonies formed per cells plated. Percentage of actively cycling HPC was estimated from cell loss due to suicidal uptake of tritiated thymidine, as described previously [25]. Colonies were scored by two blinded readers (Figure S4) after 7-day incubation at 37°C with 5% O_2 and 5% CO_2.

Phenotypic Analysis of murine BM Stem and Progenitor Cells and human ASC

The following stem and progenitor cell populations were phenotypically identified in the BM: lineage$^-$Sca1$^+$c-Kit$^+$ cells (LSK, enriched for hematopoietic stem and progenitor cells), long-term HSC (LT-HSC, CD34$^-$CD135$^-$ LSK), short-term HSC (ST-HSC; CD34$^+$CD135$^-$ LSK), multi-potent progenitors (MPP; CD34$^+$CD135$^+$ LSK), common myeloid progenitor (CMP; Lin$^-$Sca1$^-$c-Kit$^+$CD34$^+$FcγR^{low}), and granulocyte/macrophage progenitor (GMP; Lin$^-$Sca1$^-$c-Kit$^+$CD34$^-$FcγR$^+$) (Figure S1B). BM was collected and stained with antibodies to surface markers as previously described [26, 27]. Anti-mouse antibodies c-Kit, Sca1, FcγR, IL7Rα, Lineage Cocktail, and isotype controls were purchased from BD Biosciences. Anti-mouse CD34 antibody was purchased from eBioscience. Experiments were performed on a LSR II (BD Biosciences, San Jose, CA, http://www.bdbiosciences.com/) instrument

and data was analyzed using Flowjo software (Tree Star, Ashland, OR, http://www.treestar.com/). Antibodies used to identify human ASC, including CD10, CD44, CD90, CD73, CD105, CD31, CD45, and CD106 were purchased from BD Biosciences.

RNA Extraction and Quantitative Real-Time PCR

Whole lungs were perfused free of blood via right ventricular perfusion with 10 ml warmed saline, rapidly excised en bloc, blotted, and snap-frozen in liquid nitrogen. Total RNA was extracted from lung homogenates using the RNeasy mini kit (Qiagen, Venlo, Limburg, http://www.qiagen.com/) following manufacturer's instructions. Reverse transcription with High-Capacity cDNA Archive Kit (Applied Biosystems) and real-time PCR with SYBR Green Master Mix (Applied Biosystems) and glyceraldehyde 3-phosphate dehydrogenase (GAPDH) as an internal control were carried out as previously described [18].

DNA Extraction and Real-time PCR for human Alu sequences

Total bone marrow cells were harvested from both femurs of mice receiving 3×10^6 hASC i.v. two days before harvest using Wizard Genomic DNA purification kit (Promega, Madison, WI) following manufacturer's instructions. Real-time PCR for human Alu sequences was performed as previously described.[22] Standard curves were generated by adding serial dilutions of hASC into murine bone marrow samples before homogenization.

Gene expression analysis based on RT^2 PCR assay

BM LSK cells from mice exposed to ambient air or CS for 7 weeks, with or without i.v. hASC (3×10^5 weekly) treatment were sorted on Reflection II (BD Biosciences). Total RNA was isolated with RNeasy mini kit (Qiagen), according to the manufacturer protocol. Gene expression of LSK cells were analyzed using the Mouse Signal Transduction Pathway Finder™ RT^2 *profiler*™ PCR Array (PAMM-014) (Qiagen). This array was chosen to identify genes in selected signal transduction pathways that are influenced by CS and hASC. Quality control was performed on all RNA samples with the RT^2 RNA QC PCR Arrays (Qiagen). Complementary DNA was prepared from RNA using RT^2 First Strand Kit and amplified by real time PCR using SuperArray RT^2 qPCR Master Mix on ABI StepOnePlus (Applied Biosystems). Differential gene expression and statistical analysis of data were done using the SuperArray software.

TSG-6 ELISA

Levels of TSG-6 protein in the medium collected from hASC were determined by ELISA as previously described with modifications [22]. A 96-well plate (Maxisorp; Nunc) was coated with 50 μl of 10 μg/ml TSG-6 antibody (clone A38.1.20; Santa Cruz Biotechnology) in 0.2 M sodium bicarbonate buffer (pH 9.2) overnight at 4°C. Plates were washed with washing buffer (R&D systems) after this and all subsequent steps. Nonspecific sites were blocked with 0.25% BSA in PBS/0.05% Tween (blocking buffer) for 1 hr at room temperature. Samples of 50 μl or standards of rhTSG-6 protein (R&D systems) in dilution buffer were added and incubated for 2 hrs at room temperature, followed by 50 μl/well of 0.5 μg/ml biotinylated anti-hTSG-6 antibody (R&D systems) in blocking buffer for 2 hrs at room temperature. Bound antibody was detected by incubation for 20 min with streptavidin-

horseradish peroxidase (R&D systems), diluted 1:200 in PBS and then with substrate solution (R&D systems) for 20 min. Absorbance at 450 nm and 584 nm was measured by spectrophotometer (SpectraMax M5; Molecular Devices, Sunnyvale, CA, http://www.moleculardevices.com/).

Transfection of hASC with TSG-6 siRNA

Human ASC were plated at 200 cells/cm^2 in EGM2MV media (Lonza) lacking antibiotics. Once 40% confluent, cells were transfected with siRNA for TSG-6 or scramble control siRNA (Santa Cruz Biotechnology, Santa Cruz, CA, http://www.scbt.com/) with a Lipofectamine RNAiMAX (Invitrogen, Carlsbad, CA, http://www.lifetechnologies.com/invitrogen). For each 150 mm flask, a mixture of 36 μl siRNA (10 μM), 45 μl RNAiMAX, and 3 ml OptiMEM I Medium (Invitrogen) was incubated for 20 min at room temperature and then diluted by 10 fold with OptiMEM I medium (Gibco, Langley, OK, http://www.lifetechnologies.com/) before adding to the cells. After incubation for 6 hrs, the medium was replaced with 30 ml EGM2MV. To confirm knockdown of TSG-6, TSG-6 protein in cell culture supernatant was assayed by ELISA.

Statistical Analyses

Data are shown as mean ± SEM. Comparisons between two groups were made with the use of ANOVA and Newman-Keuls post-hoc analysis. A p value of < 0.05 was considered significant. Correlation coefficients for the changes in transcript expression displayed in Figure 7 were calculated based on the relative ratio of each evaluated transcript between air (AC) and smoking (CS + PBS) exposure groups (x value); and between smoking with (CS + ASC) or without hASC (CS + PBS) administration groups (y value) using the following formula (n = 84 or 19 molecules of interest),

$$r=[n(\sum xy)-(\sum x)(\sum y)]/\sqrt{[n\sum x^2-(\sum x)^2]|[n\sum y^2-(\sum y)^2])}.$$

Results

Acute reduction and slow recovery of HPC clonogenicity after CS and normalization by hASC

Previous work has documented a decline of BM myeloid progenitors in BALB/c mice upon 3 week long exposure to CS [17]. Our results identified the onset of CS-induced myelosuppression in C57BL/6 mice after CS exposure for only 3 days, by which time total CFU-GM, BFU-E, and CFU-GEMM per femur significantly declined by approximately 40%, 55% and 50%, respectively (Figure 1). These progenitor subsets were found to differ both in their sensitivity to CS and with respect to their rate of post-CS recovery, with BFU-E and CFU-GEMM recovering more slowly after CS cessation. Given our previous data demonstrating that repetitive administration of murine ASC reversed systemic CS toxicity in mice following chronic CS exposure, we tested whether a single i.v. injection of xenogeneic hASC could rescue HPC function in this model of short-term CS exposure. To mimic the provision of cells to patients with smoking history, cells were administered near the midpoint of the CS period (on Day 2 of 3-day CS exposure). Remarkably, hASC restored

the frequency of all 3 classes of progenitors close to the baseline nonsmoker levels (Figure 1).

hASC restored depleted LSK cells following prolonged CS exposure

The rapid (within 3 days) CS-induced loss of functional progenitors, as defined by clonogenic capacity, occurred without detectable changes in either total BM cellularity (Figure 2A) or LSK cells (a population enriched in HSC and HPC, Figure 2B). Given the evident defect in myeloid colony formation, we also examined early and late myeloid progenitors defined by flow cytometry using standard phenotypic profiles (MPP, CMP, and GMP). Interestingly, while the number of these progenitors remained unchanged, the number of LT-HSC increased upon CS exposure for 3 days (Figure S1), possibly representing an early adaptive response by more primitive hematopoietic cells to compensate for the loss of more mature hematopoietic cells. This notion is supported by the observation that the repository of more mature LSK cells was temporarily maintained during the 3 days of CS exposure; however, the compensation was transient, and LSK numbers were markedly reduced (by nearly 60%) upon extension of CS exposure time to 7 weeks. Consistent with findings in the 3 day model, weekly injection of hASC was able to fully restore the number of LSK cells to the level of nonsmoking mice (Figure 2B).

Injected hASC are not localized in mouse BM

To test for the presence of BM-localized hASC as possibly underlying the therapeutic effects of hASC observed above, immunocompromised NSG mice were exposed to 6 months of CS and received 3×10^5 hASC i.v. weekly during the last 4 months (to increase possible BM accumulation of hASC). Total BM cells were isolated and plated for 7 days, and adherent cells were evaluated by anti-human nuclei antibody staining. Remarkably, no human cells were detected (Figure S2), supporting the notion that hASC affect the HPC remotely via paracrine factors.

hASC respond to CS-induced host inflammatory cytokines by secretion of TSG-6

CS is typically associated with increased release of proinflammatory cytokines [28]. We have previously shown that i.v. injected hASC are transiently trapped in the lung [18]. To test whether pulmonary hASC secrete TSG-6 in the context of CS-induced host responses, we measured expression of murine TNFα and IL1β reflecting host inflammation and human TSG-6 reflecting hASC activity in the lung after C57BL/6 mice were exposed to 3-day CS and received either 3×10^5 hASC i.v. or vehicle on Day 2. We observed a marked increase of TNFα (4.1 fold) and IL1β (3.9 fold) transcripts in lungs exposed to 3-day CS (Figure 3A). Using human-specific TSG-6 primers, we detected high levels of human TSG-6 transcripts in lungs from mice harboring hASC (Figure 3B). To further evaluate the key host pro-inflammatory signals important to provoke this response in hASC, we measured secretion of TSG-6 from hASC exposed *in vitro* to TNFα, IL1β, or IFNγ. After incubation with 20 ng/ml human TNFα or IL1β for 24 hours, TSG-6 secretion increased from undetectable levels to over 5.0-8.7 ng/10^3 cells in 24 hrs (Figure 3C); in contrast, no induction was seen in response to IFNγ. Moreover, in parallel experiments, mouse TNFα or IL1β demonstrated equivalent stimulatory effects on hASC (Figure 3D), confirming the ability of the

xenogeneic human cells to respond to the murine host environment, leading to induction of TSG-6 secretion.

TSG-6 knockdown in hASC by siRNA

To determine the role of TSG-6 secretion for hASC effects on HPC, silencing of *TSG-6* expression using siRNA construct was performed. *TSG-6* siRNA transfection yielded a decrease in secretion of TSG-6 protein (Figure 4A), in the presence of TNFα stimulation for 24 hrs, by more than 80%; whereas scrambled control RNA exposure did not affect TSG-6 secretion significantly by comparison with non-transfected control cells. Extended incubation of hASC in EBM2 medium after washing demonstrated persistence of the TNFα stimulation as well as *TSG-6* siRNA interference for at least 24 hrs (Figure 4B). This method of generating conditioned media from control and *TSG-6* siRNA exposed hASC, allowed for a direct comparison of their efficacy while minimizing confounding effects by admixed TNFα and siRNA.

TSG-6 is a key mediator for myeloprotective effects of hASC

To determine the role of TSG-6 in the myeloprotective effect of hASC *in vivo*, equal amounts (3×10^5) of hASC either non-transfected, or transfected with TSG-6 siRNA or scrambled siRNA were administered i.v. on Day 2 of 3-day CS exposure. Analysis of BM on Day 4 revealed that both non-transfected and scrambled siRNA-transfected hASC were capable of reversing the significant decrease of CFU-GM (Figure 5A) and BFU-E (Figure 5B) subsequent to CS, while transfection of hASC with TSG-6 siRNA nearly completely abrogated their therapeutic effect. Changes of CFU-GEMM were not statistically significant due to greater variability, but displayed the same trend as CFU-GM and BFU-E (Figure 5C). These results suggest that TSG-6 is a key mediator of myeloprotective functions of hASC *in vivo*.

TSG-6 antagonizes CSE-induced myelosuppression *in vitro*

TSG-6 may attenuate the CS-induced myelosuppression by either counteracting the biological effect of CS on HPC, or by inhibiting the release of endogenous mediators such as TNFα that could affect hematopoiesis. We established an *in vitro* model using soluble CS extract (CSE), to mimic the mixture of potential circulating compounds derived from CS. In accordance with myelosuppression observed *in vivo*, CFU-GM *in vitro* was decreased by 75% after treatment with 1.5% CSE for 7 days. This direct suppressive effect of CS-derived compounds was fully ameliorated by co-cultured hASC as well as hASC-conditioned media (ASC-CM), and partially attenuated by rhTSG-6 protein (0.5 μg/ml), but not by conditioned media from hASC in which TSG-6 secretion was silenced (Figure 5D). These data support that in addition to its known anti-inflammatory effect, TSG-6 directly antagonizes the myelosuppressive effect of CS and is necessary for the effect of the hASC secretome in this *in vitro* model.

ASC-CM as well as TSG-6 reproduce effects of hASC *in vivo*

To further test the notion that conditioned medium and soluble factors such as TSG-6 contribute importantly to the effects of hASC *in vivo*, we next evaluated the effect of ASC-

CM in comparison to that of the *in vivo* administration of hASC. Conditioned media from TNFα-activated wild type hASC fully recapitulated the *in vivo* therapeutic effect of hASC themselves. In contrast, when TSG-6 was knocked down in hASC before media was conditioned, the efficacy of ASC-CM was also reduced. The effect of TSG-6 knockdown in hASC used to condition media was overcome by addition of soluble rhTSG-6 to the defective conditioned media. Notably, rhTSG-6 protein alone was able to achieve the same effect as hASC and ASC-CM (Figure 6A). Consistent with this observation, even more prominent changes were observed in the actively cycling HPC (Figure 6B). These data suggest that TSG-6 is a critical component underlying the activity of hASC-CM.

Multiple alterations in HSC/HPC signaling are induced by CS and reversed by hASC

In order to unveil possible mechanisms for CS and hASC effects on BM HSC/HPC, we performed pathway-focused RT-PCR array analysis in LSK cells (enriched for HSC/HPC) from mice in 3 treatment groups (n = 3/group). Exposure to CS for 7 weeks was associated with a 2.8-fold increase ($p < 0.05$) in the expression of *Lfng*, the transcript of the Lunatic Fringe protein, which is known to inhibit binding of Jagged1 while promoting binding of delta-like ligand to the Notch1 receptor. Interestingly, ASC exposure reversed this effect ($p < 0.05$), supporting a potentially significant role of *Notch* signaling in these complementary effects. In addition, CS exposure resulted in greater than two-fold down-regulation of six genes (*Cebpd, Bcl-x, Wnt2b, Wnt6, Hmox1*, and *Tnfsf10*); remarkably, each of these decreases was reversed by more than two-fold after hASC treatment (Figure 7). Similarly, another gene, *Gsr*, implicated in oxidative stress, was noted to be up-regulated by CS and restored towards baseline levels by hASC (Table S2). While the latter alterations displayed trends individually, the results taken together strongly support a consistently antagonistic effect of hASC against molecular consequences of CS exposure across multiple pathways (correlation coefficient for alteration ratio = 0.797 for all 84 molecular species measured; correlation coefficient 0.936 if only counting molecules with > 2 fold change by either CS or hASC treatment). Pathways and molecules demonstrating at least twofold changes upon either treatment include *Notch1* (*Jag1* and *Lfng*), *STAT3* (*Cebpd, Bcl2l1, and Lrg1*), *Hedgehog* (*Wnt2b, Wnt6, Axin2,* and *Ppard*), oxidative stress (*Sqstm1* and *Gsr*), *p53* (*Fas, Bax,* and *Btg2*), *TGFβ* (*Tnfsf10, Atf4,* and *Cdkn1b*), and hypoxia responses (*Vegfa* and *Hmox1*).

Discussion

The multi-organ detrimental effects of CS have previously been attributed to systemic inflammation, oxidative stress, endothelial injury, and hemodynamic dysfunction [29-33]. Little attention has been paid to the involvement of HPC in the pathogenesis of smoking-related diseases. We hypothesized that CS-induced damage to bone marrow progenitors might in fact represent an early manifestation of CS toxicity. Our study confirmed this hypothesis, demonstrating an acute onset (3 days of CS exposure) of CS-induced suppression of clonogenic activity of selected progenitors (BFU-E and CFU-GEMM), persistent for greater than 1 week; this precedes the development of detectable pulmonary emphysema, typically requiring 4-6 months. Notably, the early pathological changes in HPC clonogenic function were not manifested in phenotypic enumeration of LSK cells until

several weeks later. Such a temporal discrepancy between functional and phenotypic observations has also been noted previously, supporting clonogenic assays as a more sensitive method to detect early hematopoietic alterations [27]. It is notable that the decline of LSK numbers after 7 weeks of CS exposure implies a potential harmful effect of CS on HSC, which corroborates the clinically observed correlation between smoking history and worse prognosis following BM transplantation [14]. We recognize that these findings from this study provide only indirect insight into the effect of CS on the functionality of HSC and that future BM transplantation studies will be required for further direct characterization. Given the emerging understanding of the importance of BM progenitor cells for peripheral tissue regeneration, it may be speculated that an ongoing CS-induced deficiency of BM-derived cells important to extramedullary repair contributes critically to the pathogenesis of numerous diseases related to CS.

CS has multiple impacts on the immune system, which may in turn affect other organ systems secondarily [34, 35]. Accordingly, to better mimic human CS-induced disease, we employed immune-competent mice in this study. We chose to probe the mechanisms of ASC activity using human-derived ASC, in light of several considerations: 1) the recognition that mesenchymal stromal cells, including ASC, lack HLA-DR antigen and are immune-privileged [36]; 2) a majority of cells disappear from the host environment within days after systemic administration [22]; 3) hASC have exhibited potent cross-species paracrine activities in multiple disease models [37]; and 4) findings from hASC can be more easily translated into future clinical applications.

Key therapeutic effects of intravenously delivered cells may arise from factors released systemically by cells trapped in the lung acting in a paracrine fashion rather than by direct cell replacement. A seminal study demonstrated that a similar type of mesenchymal population, MSC derived from BM, was able to secrete TSG-6 when trapped in the lung and exposed to TNFα.[22] Our observation of an acute increase of inflammatory cytokine expression in lung after CS exposure prompted our hypothesis that TSG-6 might play a role in the effects of hASC to ameliorate CS-induced pathology in *vivo*. Indeed, our data clearly show that hASC not only respond to TNFα but also to other inflammatory stimuli such as IL1β; and that this response occurs in the context of xenotransplantation. We found for the first time that the activity of hASC to markedly rescue hematopoiesis are replicated by conditioned media generated in response to TNFα; and identified TSG-6 as both necessary and sufficient to explain the paracrine effect of hASC in the CS-induced myelosuppression model. These data provide a basis for the notion of exploring off-the-shelf cell-derived, yet acellular, medical products of hASC, at least for selected indications.

The discovery of myeloprotective activity of TSG-6 is novel information and provides a strong basis for future explorations of its application to other circumstances such as irradiation or chemotherapy-induced myelosuppression. The precise mechanisms by which this effect of TSG-6 occurs remain to be determined. Potent anti-inflammatory effects of TSG-6 have been demonstrated in multiple disease models [38-40]. Among the proposed mechanisms of action is binding to CD44 and interfering with NF-κb signaling pathway in macrophages to suppress TNFα secretion [21]. A contribution of anti-inflammatory effect of TSG-6 to its overall benefit in the smoking model is possible, based on the observed decline

of TNFα expression in lungs treated with hASC. Although pro-inflammatory cytokines such as TNFα can contribute to inhibition of hematopoiesis [41], our *in vitro* model of CSE-induced progenitor suppression suggests that important adverse effects on hematopoiesis also involve direct toxicity of compounds present in CS, which are ameliorated by hASC.

Pathway analysis of genes within BM LSK cells further confirmed our hypothesis that hASC are capable of reversing CS-induced changes, such as the down-regulation of the gene Lunatic fringe (*Lfng*), a critical mediator of the Notch signaling pathway. Notch signaling plays a crucial role in the regulation of hematopoietic stem and progenitor cells in adult hematopoiesis [42]. *Lfng* has been shown to enhance competitive binding of delta-like ligand to *Notch1* receptor (instead of *Jagged1* ligand), which has been associated with inhibition of colony formation from HPC, especially in the presence of stem cell factor [43, 44]. Interestingly, Notch alterations due to CS exposure may not be restricted to BM but rather represent a general host response, since Notch modulation has also been reported in human lung epithelial cells in the context of CS-induced COPD [45]. Notably, Cdkn1b (p27), a key molecule in the TGFβ signaling pathway, demonstrated a trend of up-regulation by CS and down-regulation by ASC. This observation is in concert with the previous demonstration of its inhibitory role in the proliferation of hematopoietic progenitors, [46] and could represent one pathway which mediates the observed decrease in HPC cycling and total numbers. In contrast, Tnfsf10 (Tumor-necrosis-factor-related apoptosis-inducing ligand, TRAIL) demonstrated a trend of decrease by CS. This alteration, even if validated, may be physiologically less significant since nonmalignant murine bone marrow hematopoietic progenitors are resistant to TRAIL-induced apoptosis. [47] Overall, signaling molecules involved in multiple pathways were found to consistently exhibit trends of alterations occurring as a result of CS that were reversed in direction by hASC treatment. Due to the limited available sample size, several such alterations individually did not reach statistical significance; yet the correlation among the multiple alterations by CS and their negation by hASC was quite strong, and may warrant future evaluation of these pathways to reveal additional mechanisms underlying CS-induced pathology and the ameliorating effects of hASC.

Conclusion

This study addressed three major research questions: the chronology of CS-induced BM dysfunction, the therapeutic value of hASC, and the identity of a key mediator responsible for the activity of hASC on murine hematopoiesis. Our study demonstrated that acute exposure to cigarette smoke promptly induces a clonogenic defect of BM progenitors with subsequent reduction of phenotypic (LSK) HSC/HPC, and that this myelotoxicity of CS can be successfully reversed by xenogeneic hASC. We discovered that this robust activity was recapitulated by conditioned medium derived from hASC, as well as by hTSG-6 protein, which is secreted by ASC in the context of CS exposure. We further established that TSG-6 was both necessary and sufficient as a mediator for the myeloprotective activity of hASC and hASC-CM. To our knowledge, this is the first evidence for a myeloprotective effect of TSG-6, which traditionally has been recognized as an anti-inflammatory protein. These observations, in conjunction with the demonstration of ASC-mediated reversal of multiple CS-induced changes of regulatory signaling molecules, support the concept that hASC,

hASC-CM and TSG-6 represent promising approaches to combat the myelotoxicity of CS. Our findings provide a novel mechanistic perspective relating bone marrow function to the pathogenesis and treatment of smoking-related diseases, and may also have more general implications for the future enhancement of deranged hematopoiesis by ASC and TSG-6.

Supplementary Material

Refer to Web version on PubMed Central for supplementary material.

Acknowledgments

This work was supported by the National Institutes of Health (1R01HL105772-01A1, K.L.M. and I.P.), American Heart Association (11PRE5730005, J.X.), Roudebush VA Center for Regenerative Medicine, and the Cryptic Masons Medical Research Foundation. We thank Louis M. Pelus for helping with BM cell counts. We also thank Giao Hangoc and Scott H. Cooper for helping to set up colony-forming-unit assays.

DJP is chair of the scientific advisory committee of a biotech company (Temple Therapeutics LLC) with no funds related to this study.

References

1. Weiss L, Geduldig U. Barrier cells: stromal regulation of hematopoiesis and blood cell release in normal and stressed murine bone marrow. Blood. 1991; 78:975–990. [PubMed: 1868254]
2. De Toni F, Poglio S, Youcef AB, et al. Human adipose-derived stromal cells efficiently support hematopoiesis in vitro and in vivo: a key step for therapeutic studies. Stem Cells Dev. 2011; 20:2127–2138. [PubMed: 21388235]
3. Han J, Koh YJ, Moon HR, et al. Adipose tissue is an extramedullary reservoir for functional hematopoietic stem and progenitor cells. Blood. 2010; 115:957–964. [PubMed: 19897586]
4. Zhao L, Wei X, Ma Z, et al. Adipose stromal cells-conditional medium protected glutamate-induced CGNs neuronal death by BDNF. Neuroscience letters. 2009; 452:238–240. [PubMed: 19348731]
5. Cai L, Johnstone BH, Cook TG, et al. Suppression of hepatocyte growth factor production impairs the ability of adipose-derived stem cells to promote ischemic tissue revascularization. Stem Cells. 2007; 25:3234–3243. [PubMed: 17901400]
6. Erhardt L. Cigarette smoking: an undertreated risk factor for cardiovascular disease. Atherosclerosis. 2009; 205:23–32. [PubMed: 19217623]
7. Hecht SS. Cigarette smoking: cancer risks, carcinogens, and mechanisms. Langenbeck's archives of surgery / Deutsche Gesellschaft fur Chirurgie. 2006; 391:603–613.
8. Patel RR, Ryu JH, Vassallo R. Cigarette smoking and diffuse lung disease. Drugs. 2008; 68:1511–1527. [PubMed: 18627208]
9. Nagasawa Y, Yamamoto R, Rakugi H, et al. Cigarette smoking and chronic kidney diseases. Hypertension research : official journal of the Japanese Society of Hypertension. 2012; 35:261–265. [PubMed: 22158113]
10. Corpechot C, Gaouar F, Chretien Y, et al. Smoking as an independent risk factor of liver fibrosis in primary biliary cirrhosis. Journal of hepatology. 2012; 56:218–224. [PubMed: 21703179]
11. Jafari N, Hintzen RQ. The association between cigarette smoking and multiple sclerosis. Journal of the neurological sciences. 2011; 311:78–85. [PubMed: 21975015]
12. Soares SR, Melo MA. Cigarette smoking and reproductive function. Current opinion in obstetrics & gynecology. 2008; 20:281–291. [PubMed: 18460944]
13. Mehta H, Nazzal K, Sadikot RT. Cigarette smoking and innate immunity. Inflammation research : official journal of the European Histamine Research Society “et al“. 2008; 57:497–503. [PubMed: 19109742]

14. Ehlers SL, Gastineau DA, Patten CA, et al. The impact of smoking on outcomes among patients undergoing hematopoietic SCT for the treatment of acute leukemia. Bone Marrow Transplant. 2011; 46:285–290. [PubMed: 20479707]
15. Serobyan N, Orlovskaya I, Kozlov V, et al. Exposure to nicotine during gestation interferes with the colonization of fetal bone marrow by hematopoietic stem/progenitor cells. Stem Cells Dev. 2005; 14:81–91. [PubMed: 15725747]
16. Pandit TS, Sikora L, Muralidhar G, et al. Sustained exposure to nicotine leads to extramedullary hematopoiesis in the spleen. Stem Cells. 2006; 24:2373–2381. [PubMed: 16825610]
17. Khaldoyanidi S, Sikora L, Orlovskaya I, et al. Correlation between nicotine-induced inhibition of hematopoiesis and decreased CD44 expression on bone marrow stromal cells. Blood. 2001; 98:303–312. [PubMed: 11435297]
18. Schweitzer KS, Johnstone BH, Garrison J, et al. Adipose stem cell treatment in mice attenuates lung and systemic injury induced by cigarette smoking. American journal of respiratory and critical care medicine. 2011; 183:215–225. [PubMed: 20709815]
19. Kota DJ, Wiggins LL, Yoon N, et al. TSG-6 produced by hMSCs delays the onset of autoimmune diabetes by suppressing Th1 development and enhancing tolerogenicity. Diabetes. 2013
20. Danchuk S, Ylostalo JH, Hossain F, et al. Human multipotent stromal cells attenuate lipopolysaccharide-induced acute lung injury in mice via secretion of tumor necrosis factor-alpha-induced protein 6. Stem Cell Res Ther. 2011; 2:27. [PubMed: 21569482]
21. Choi H, Lee RH, Bazhanov N, et al. Anti-inflammatory protein TSG-6 secreted by activated MSCs attenuates zymosan-induced mouse peritonitis by decreasing TLR2/NF-{kappa}B signaling in resident macrophages. Blood. 2011
22. Lee RH, Pulin AA, Seo MJ, et al. Intravenous hMSCs improve myocardial infarction in mice because cells embolized in lung are activated to secrete the anti-inflammatory protein TSG-6. Cell stem cell. 2009; 5:54–63. [PubMed: 19570514]
23. Traktuev DO, Merfeld-Clauss S, Li J, et al. A population of multipotent CD34-positive adipose stromal cells share pericyte and mesenchymal surface markers, reside in a periendothelial location, and stabilize endothelial networks. Circ Res. 2008; 102:77–85. [PubMed: 17967785]
24. Broxmeyer HE, Orschell CM, Clapp DW, et al. Rapid mobilization of murine and human hematopoietic stem and progenitor cells with AMD3100, a CXCR4 antagonist. The Journal of experimental medicine. 2005; 201:1307–1318. [PubMed: 15837815]
25. Cooper S, Broxmeyer HE. Clonogenic methods in vitro for the enumeration of granulocytemacrophage progenitor cells (CFU-GM) in human bone marrow and mouse bone marrow and spleen. J of Tissue Cult Methods. 1991; 13:77–82.
26. Kobayashi M, Srour EF. Regulation of murine hematopoietic stem cell quiescence by Dmtf1. Blood. 2011; 118:6562–6571. [PubMed: 22039255]
27. Rohrabaugh SL, Hangoc G, Kelley MR, et al. Mad2 haploinsufficiency protects hematopoietic progenitor cells subjected to cell-cycle stress in vivo and to inhibition of redox function of Ape1/Ref-1 in vitro. Experimental hematology. 2011; 39:415–423. [PubMed: 21216274]
28. Braber S, Henricks PA, Nijkamp FP, et al. Inflammatory changes in the airways of mice caused by cigarette smoke exposure are only partially reversed after smoking cessation. Respir Res. 2010; 11:99. [PubMed: 20649997]
29. Lee J, Taneja V, Vassallo R. Cigarette smoking and inflammation: cellular and molecular mechanisms. Journal of dental research. 2012; 91:142–149. [PubMed: 21876032]
30. Grassi D, Desideri G, Ferri L, et al. Oxidative stress and endothelial dysfunction: say NO to cigarette smoking! Current pharmaceutical design. 2010; 16:2539–2550. [PubMed: 20550504]
31. Csiszar A, Podlutsky A, Wolin MS, et al. Oxidative stress and accelerated vascular aging: implications for cigarette smoking. Frontiers in bioscience : a journal and virtual library. 2009; 14:3128–3144.
32. Cacciola RR, Guarino F, Polosa R. Relevance of endothelial-haemostatic dysfunction in cigarette smoking. Current medicinal chemistry. 2007; 14:1887–1892. [PubMed: 17627524]
33. Michael Pittilo R. Cigarette smoking, endothelial injury and cardiovascular disease. International journal of experimental pathology. 2000; 81:219–230. [PubMed: 10971743]

34. Hagiwara E, Takahashi KI, Okubo T, et al. Cigarette smoking depletes cells spontaneously secreting Th(1) cytokines in the human airway. Cytokine. 2001; 14:121–126. [PubMed: 11356013]

35. Hersey P, Prendergast D, Edwards A. Effects of cigarette smoking on the immune system. Follow-up studies in normal subjects after cessation of smoking. The Medical journal of Australia. 1983; 2:425–429. [PubMed: 6633406]

36. Griffin MD, Ritter T, Mahon BP. Immunological aspects of allogeneic mesenchymal stem cell therapies. Human gene therapy. 2010; 21:1641–1655. [PubMed: 20718666]

37. Marconi S, Castiglione G, Turano E, et al. Human adipose-derived mesenchymal stem cells systemically injected promote peripheral nerve regeneration in the mouse model of sciatic crush. Tissue engineering Part A. 2012; 18:1264–1272. [PubMed: 22332955]

38. Mahoney DJ, Swales C, Athanasou NA, et al. TSG-6 inhibits osteoclast activity via an autocrine mechanism and is functionally synergistic with osteoprotegerin. Arthritis Rheum. 2011; 63:1034–1043. [PubMed: 21162099]

39. Milner CM, Higman VA, Day AJ. TSG-6: a pluripotent inflammatory mediator? Biochemical Society transactions. 2006; 34:446–450. [PubMed: 16709183]

40. Wisniewski HG, Vilcek J. TSG-6: an IL-1/TNF-inducible protein with anti-inflammatory activity. Cytokine Growth Factor Rev. 1997; 8:143–156. [PubMed: 9244409]

41. Broxmeyer HE, Williams DE, Lu L, et al. The suppressive influences of human tumor necrosis factors on bone marrow hematopoietic progenitor cells from normal donors and patients with leukemia: synergism of tumor necrosis factor and interferon-gamma. J Immunol. 1986; 136:4487–4495. [PubMed: 3086433]

42. Allman D, Aster JC, Pear WS. Notch signaling in hematopoiesis and early lymphocyte development. Immunological reviews. 2002; 187:75–86. [PubMed: 12366684]

43. Visan I, Yuan JS, Liu Y, et al. Lunatic fringe enhances competition for delta-like Notch ligands but does not overcome defective pre-TCR signaling during thymocyte beta-selection in vivo. J Immunol. 2010; 185:4609–4617. [PubMed: 20844195]

44. Ohno N, Izawa A, Hattori M, et al. dlk inhibits stem cell factor-induced colony formation of murine hematopoietic progenitors: Hes-1-independent effect. Stem cells (Dayton, Ohio). 2001; 19:71–79.

45. Tilley AE, Harvey BG, Heguy A, et al. Down-regulation of the notch pathway in human airway epithelium in association with smoking and chronic obstructive pulmonary disease. Am J Respir Crit Care Med. 2009; 179:457–466. [PubMed: 19106307]

46. Cheng T, Rodrigues N, Dombkowski D, et al. Stem cell repopulation efficiency but not pool size is governed by p27(kip1). Nature medicine. 2000; 6:1235–1240.

47. Mizrahi K, Stein J, Pearl-Yafe M, et al. Regulatory functions of TRAIL in hematopoietic progenitors: human umbilical cord blood and murine bone marrow transplantation. Leukemia. 2010; 24:1325–1334. [PubMed: 20485377]

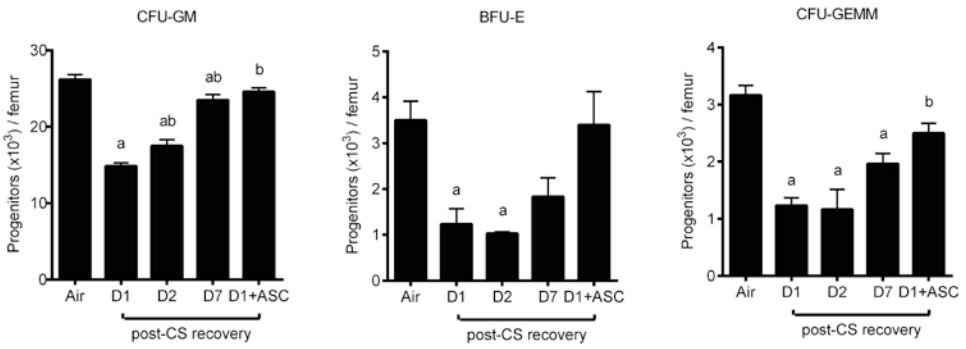

Figure 1. Recovery of mouse BM hematopoietic progenitor cells after 3-day cigarette smoking (CS) and benefit of human adipose stromal cell (hASC) treatment

C57BL/6 mice were exposed to ambient air or CS for 3 days then rested for 1-7 days (D1-D7) for recovery. One additional group received an i.v. bolus 3×10^5 hASC on Day 2 of 3-day CS and the BM was harvested one day after the last CS exposure (D1 + ASC). CFU-GM: colony forming unit- granulocyte, monocyte; BFU-E: burst forming unit-erythroid; CFU-GEMM: colony forming unit-granulocyte, erythrocyte, monocyte, and megakaryocyte. Mean ± SEM, n = 3-6/group. $^{a}p < 0.05$ (vs. air), $^{b}p < 0.05$ (vs. D1).

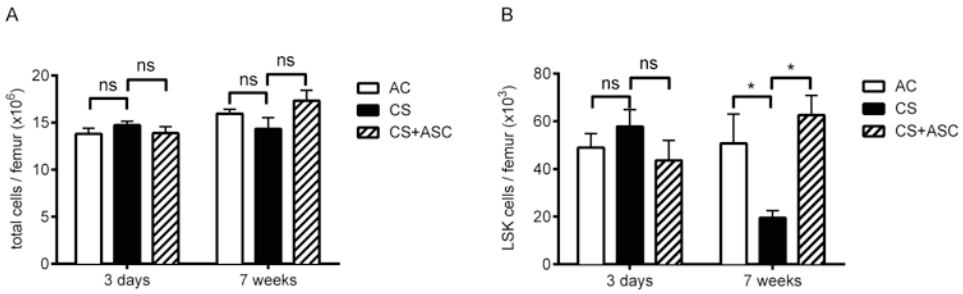

Figure 2. Prolonged CS-induced depletion of Phenotypic HSC/HPC was rescued by hASC

(A) Total BM mononuclear cells. (B) BM $Lin^{-}Sca1^{+}cKit^{+}$ (LSK) cells. For 3 day-CS mice, 3×10^5 hASC were injected i.v. on Day 2. For 7 week-CS mice, 3×10^5 hASC were injected i.v. weekly. Mean ± SEM, n = 11/group for 3-day CS, 3/group for 7-week CS; $^{*}p < 0.05$.

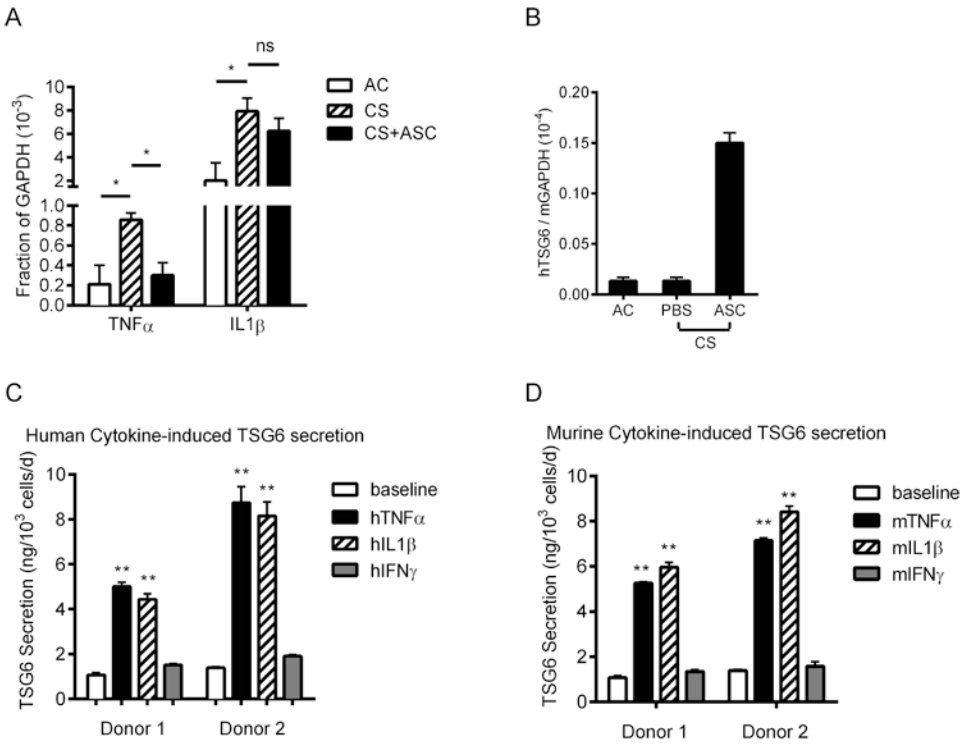

Figure 3. Inflammatory cytokines released from lungs of CS-exposed mice activated hASC to secrete TSG-6

(A) Expressions of both murine TNFα and IL1β were up-regulated in the lung after mice were exposed to 3-day CS compared to ambient air control (AC); TNFα was reduced significantly to the level of AC following i.v. injection of hASC; (B) minimum human-specific TSG-6 mRNA was detected in untreated mouse lungs, levels of which was markedly increased 40 hrs following i.v. injection of hASC; (C) In vitro, secretion of TSG-6 protein from hASC is low at baseline but strongly increased after stimulation by human pro-inflammatory cytokines (TNFα and IL1β, but not IFNγ); (D) secretion of TSG-6 from hASC can be activated similarly with cross-species mouse pro-inflammatory cytokines. Mean ± SEM, n = 3; *p < 0.05; **p < 0.01.

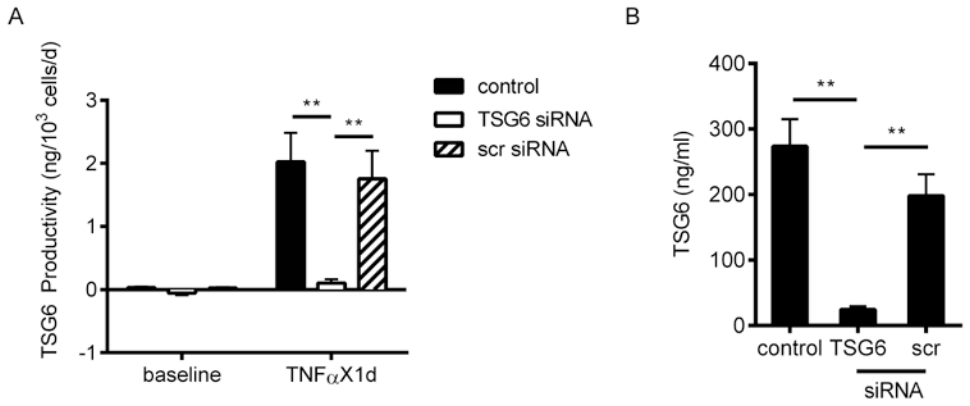

Figure 4. TSG-6 production from hASC was effectively inhibited by siRNA

(A) TSG-6 secretion from hASC not transfected (control), or transfected with TSG-6 siRNA or scrambled (scr) siRNA. Cells were incubated with or without 20 ng/ml TNFα for 24 hrs. (B) After removal of siRNA for 48 hrs and TNFα for 24 hrs, TSG-6 concentration remains significantly different in hASC-CM between non-transfected and transfected hASC. Mean ± SEM, n = 3; **p < 0.01.

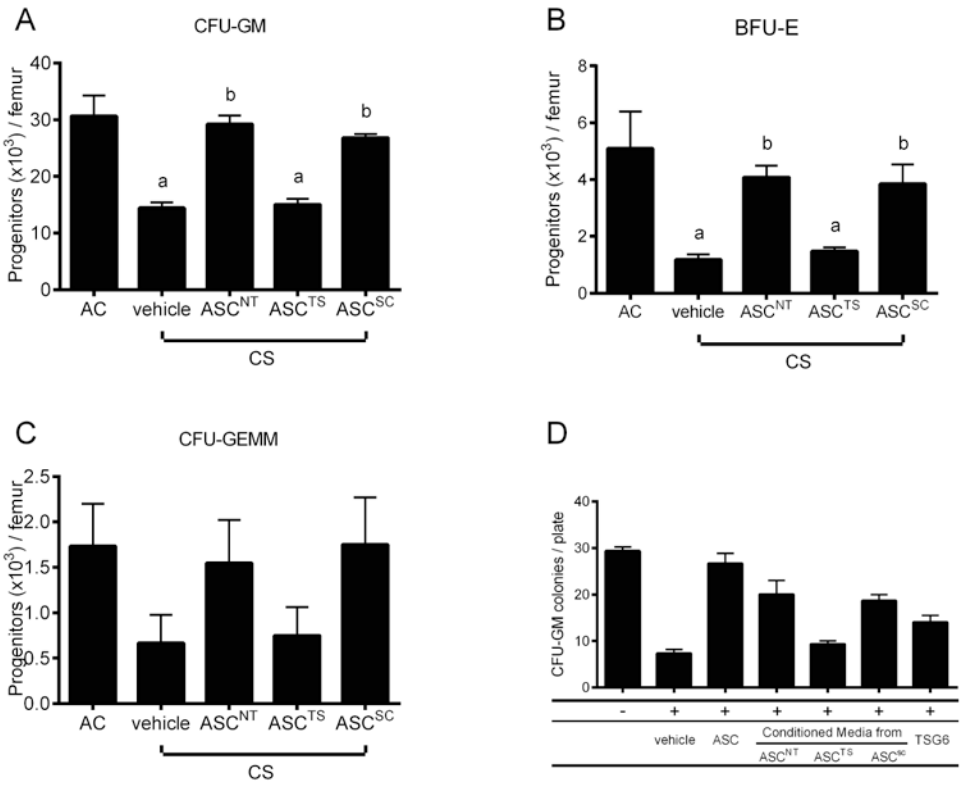

Figure 5. Myeloprotective effects of hASC were lost after TSG-6 knockdown

(A-C) C57BL/6 mice were exposed to 3-day CS and injected i.v. with 3×10^5 hASC not transfected (ASC^{NT}), transfected with TSG-6 siRNA (ASC^{TS}), or with scrambled siRNA (ASC^{SC}) on Day 2. Mean ± SEM, n = 6/group. $^{a}p < 0.05$ (vs. AC); $^{b}p < 0.05$, (vs. vehicle). (D) In vitro model of CS-induced myelosuppression demonstrating direct antagonist effects of hASC, ASC-CM, and rhTSG-6 against the toxicity of CS extract (CSE) on GM-CFU. Mouse BM cells were treated in vitro with 1.5% CSE with or without hASC ($3 \times 10^4/cm^2$) / ASC-CM (20%, v/v) / rhTSG-6 (500 ng/ml) in methylcellulose medium supplemented with FBS, mGM-CSF (10 ng/ml) & mSCF (50 ng/ml) for 7 days. Mean ± SEM, n = 3/group; $^{a}p < 0.05$, (vs. non-treated control); $^{b}p < 0.05$, vs. (CSE + vehicle). ASC^{NT} = Non-transfected ASC; ASC^{TS} = TSG-6 siRNA-transfected; ASC^{SC} = scramble siRNA-transfected.

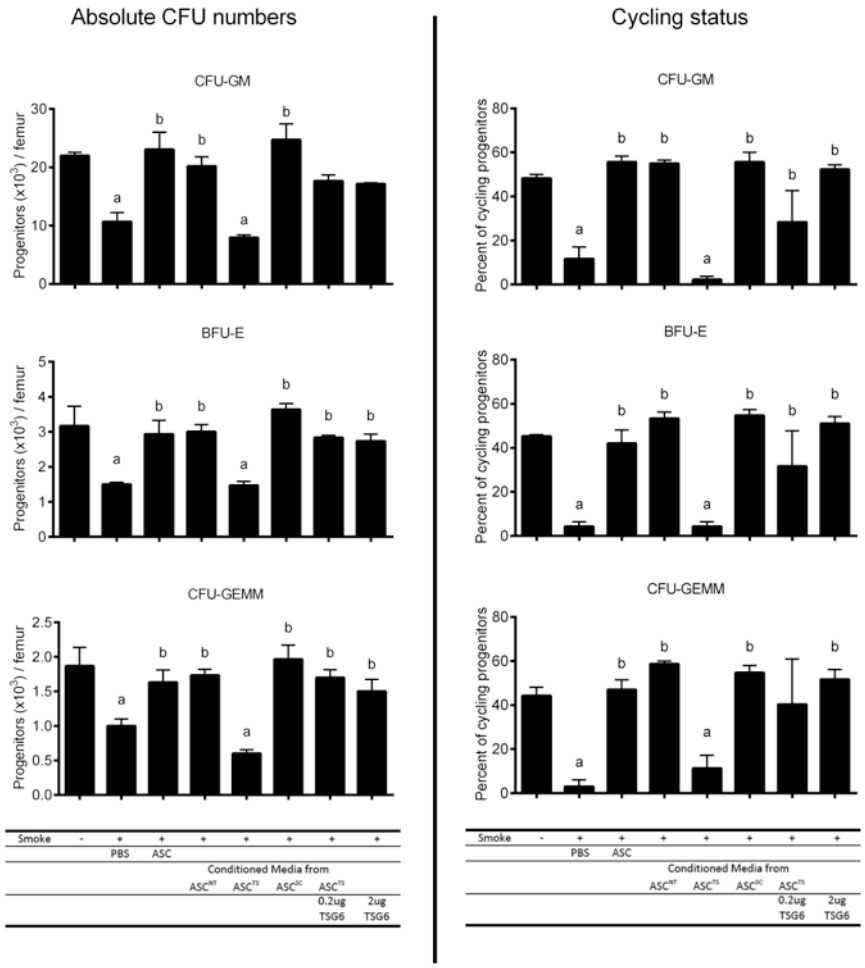

Figure 6. Effect of hASC against myelotoxicity of CS was reproduced by hASC conditioned medium as well as by TSG-6

C57BL/6 mice were exposed to ambient air or 3-day CS and injected i.v. with following treatment groups: 1) PBS; 2) 3×10^5 hASC; 3) conditioned media from non-transfected hASC(ASC^{NT}), 4) & 5) from hASC transfected with TSG-6 siRNA (ASC^{TS}) with or without supplement of 0.2 μg rhTSG-6, or 6) from hASC transfected with scrambled siRNA (ASC^{SC}); 7) 2 μg rhTSG-6. Cycling progenitors (right) demonstrates a more sensitive response to treatment than absolute number of progenitors (left). Mean ± SEM, n = 6/ group; $^{a}p < 0.05$ (vs. AC); $^{b}p < 0.05$, (vs. vehicle).

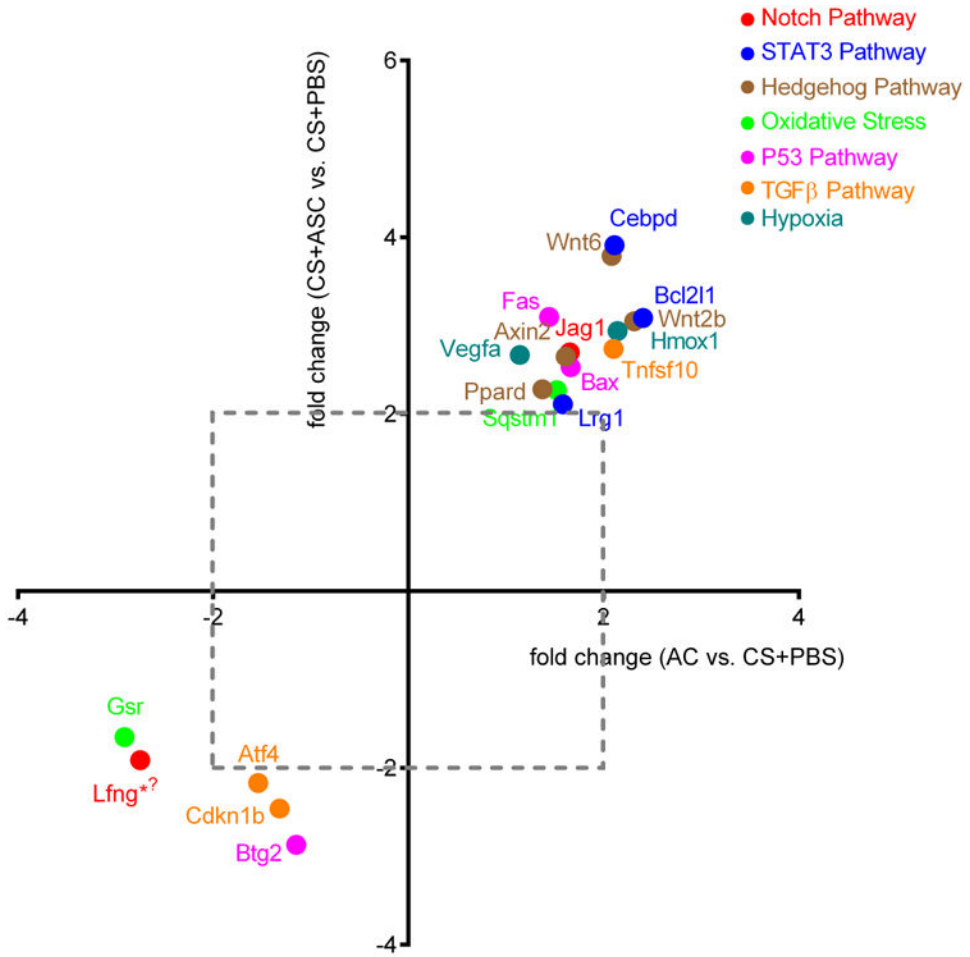

Figure 7. CS-induced changes in signaling molecules of BM LSK cells were reversed by hASC

C57BL/6 mice (n = 3/group) were exposed to ambient air (AC) or CS with (CS+ASC) or without (CS + PBS) weekly injections of hASC (3×10^5). BM LSK cells were sorted for RNA extraction. Expressions of signaling molecules were measured by real-time PCR. Positive / negative values on each axis represent fold decrease / increase between 2 comparison groups, respectively (i.e. x = 2 means two-fold greater level in AC than in CS group). Molecules downregulated or upregulated by CS and reversed by ASC are located in the upper right and lower left quadrants, respectively. Only molecules with more than two-fold changes by either treatment were displayed. *$p < 0.05$ (AC vs. CS + PBS), $^{\Phi}p < 0.05$ (CS + ASC vs. CS + PBS).